



Cite this: *Dalton Trans.*, 2014, **43**, 14284

Synthesis and thermal decomposition of a pyridylene-bridged bis- β -diketiminato magnesium hydride cluster†

Sjoerd Harder,^{*a} Jan Spielmann^b and Julia Intemann^{a,c}

Reaction of **PYR**-(Mg*n*Bu)₂, in which **PYR** is 2,6-[(DIPP)NC(Me)CHC(Me)N-]₂-pyridine and DIPP is 2,6-*i*Pr₂-phenyl, with (DIPP)NH₂BH₃ gave **PYR**-[MgNH(DIPP)BH₃]₂ (56%) which was characterized by crystal structure determination. Addition of THF resulted in β -H elimination and formation of **PYR**-[MgNH(DIPP)BH₃](MgH)·THF (57%), likewise characterized by crystal structure determination. Conversion of the second amidoborane anion in H⁻ could not be achieved. Reaction of **PYR**-(Mg*n*Bu)₂ with PhSiH₃ gave **PYR**-(MgH)₂, which crystallized as a dimer. The structure of [**PYR**-(MgH)₂]₂ shows an 8-membered ring of Mg²⁺ and H⁻ ions. Thermal decomposition at 130 °C releases one equivalent of H₂, *i.e.* 50% of the expected value. Nucleophilic attack at the *para*-position and reduction of the pyridylene bridge might explain reduced H₂ release.

Received 19th March 2014,
Accepted 11th April 2014

DOI: 10.1039/c4dt00835a

www.rsc.org/dalton

Introduction

Transition metal hydride complexes play an important role in the broader context of organometallic chemistry and have paved the way for the early development of homogeneous transition metal catalysis.¹ The extended class of late main group metal hydride compounds (*e.g.* alanes, boranes, stannanes) is also well-established and heavily used as reducing agents in organic synthesis.² The early main group metal hydrides, however, suffer from their highly polar character, which results in ionic crystal structures, (MH)_∞ and (MH₂)_∞, with very high lattice energies.^{2,3} The latter are an obstacle in the synthesis of well-defined early main group metal hydride complexes like L⁰...M-H or L⁻¹-M-H (in which L⁰ and L⁻¹ represent neutral and -1 charged ligand systems, respectively). The challenge of selectively synthesizing early main group metal hydride complexes was recently taken on, and the field is rapidly expanding.⁴⁻¹⁵ This is especially due to rewarding contributions of the field to early main group metal catalysis¹⁶⁻¹⁹ and hydrogen storage.^{11,14}

In light of this, β -diketiminato complexes of magnesium hydride (Scheme 1) have been shown to function as molecular models for the hydrogen storage system: MgH₂ \rightleftharpoons Mg +

H₂.^{11,14,20} Apart from the magnesium hydride dimer [(DIPPnacnac)MgH]₂ (Scheme 1),⁹ larger magnesium hydride clusters based on bridged β -diketiminato ligands were introduced.^{11,14} The ligand with direct connection of β -diketiminato units gave the tetranuclear magnesium hydride cluster [NN-(MgH)₂]₂.¹⁴ Using a *para*-phenylene spacer gave a larger octanuclear cluster in which MgH₂ is incorporated: [PARA-(MgH)₂]₃[MgH₂]₂ (Scheme 1).¹¹ It was shown that these magnesium hydride complexes are stable towards thermal decomposition when dissolved in aromatic solvents. However, in the solid state, thermal decomposition with release of the expected amount of H₂ is observed. As predicted by theoretical calculation,²¹ the hydrogen release temperatures (120–200 °C) are much lower than that for bulk (MgH₂)_∞ (>300 °C) and increase with the cluster size (Scheme 1).¹⁴ Hitherto, the low-valent products after H₂ elimination could not be characterized. Also, reversibility has so far not been observed.

In continuation, we extend our investigations with the 2,6-pyridylene bridged β -diketiminato ligand (**PYR**). This ligand has been shown to have unusual coordination chemistry.²²⁻²⁴ It can bridge a dimeric unit symmetrically with long, but not negligible pyridine-metal contacts (i) in Scheme 2. This leads to significant strain: the N-C-N angles in **PYR**-(Mg*n*Bu)₂ of circa 109° are much smaller than the idealized 120° value for sp² hybridization. Also asymmetric coordination modes (ii) have been observed. Due to essential free rotation of the pyridylene unit in respect of the β -diketiminato NCCC planes, another geometry with non-classic hydrogen C-H...N bonding is feasible (iii). As the bimetallic complexes **PYR**-(ZnR)₂ were found to be completely inactive in CO₂/epoxide copolymeriza-

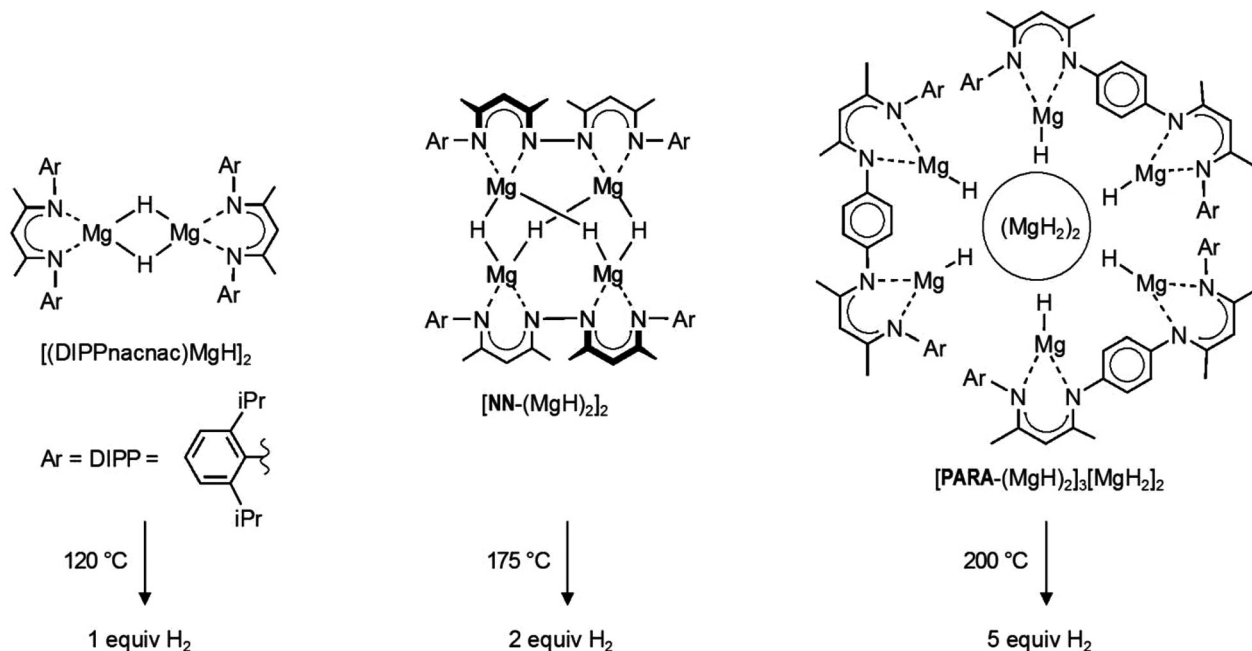
^aInorganic and Organometallic Chemistry, University Erlangen-Nürnberg, Egerlandstrasse 1, 91058 Erlangen, Germany. E-mail: sjoerd.harder@fau.de

^bInorganic Chemistry, University Duisburg-Essen, Universitätsstrasse 5, 45117 Essen, Germany

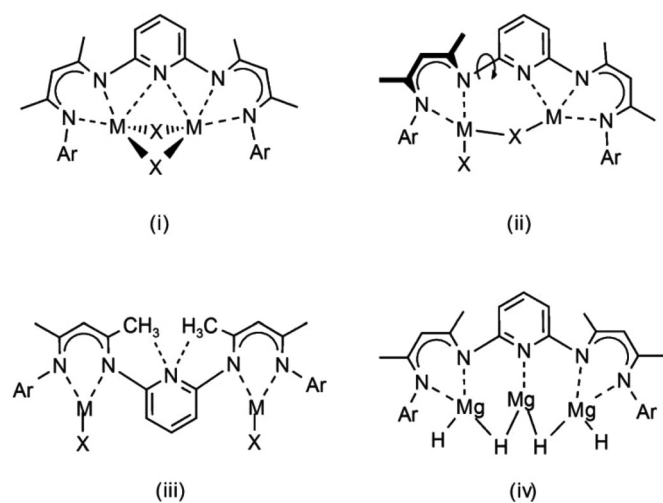
^cStratingh Institute of Chemistry, University of Groningen, Nijenborgh 4, 9747 AG Groningen, Netherlands

†CCDC 992444–992446. For crystallographic data in CIF or other electronic format see DOI: 10.1039/c4dt00835a





Scheme 1 Magnesium hydride complexes.



Scheme 2 Coordination modes of the PYR ligand.

tion, it was reasoned that such a geometry might block metal-metal communication and synergistic effects.

The pyridylene bridge in **PYR** is potentially a strongly coordinating donor that also may assist in incorporation of additional metal units: a magnesium hydride complex like (iv) could be envisioned. Here, we evaluate the magnesium hydride chemistry of the **PYR** ligand.

Results and discussion

We recently reported a convenient high-yield method for the synthesis of $[(\text{DIPPnacnac})\text{MgH}]_2$ by thermally induced $\beta\text{-H}$

elimination in the magnesium amidoborane precursor $(\text{DIPPnacnac})\text{MgNH}(i\text{Pr})\text{BH}_3$.²³ The analogue bimetallic complex $\text{PYR}[\text{MgNH}(i\text{Pr})\text{BH}_3]_2$ can be prepared according to Scheme 3, but thermal decomposition led to formation of a BNB product, presumably through an hydride intermediate.²³ We found that, in case of a 2,6- $i\text{Pr}_2\text{C}_6\text{H}_3$ substituent (DIPP) on N, the fate of thermal decomposition is different.

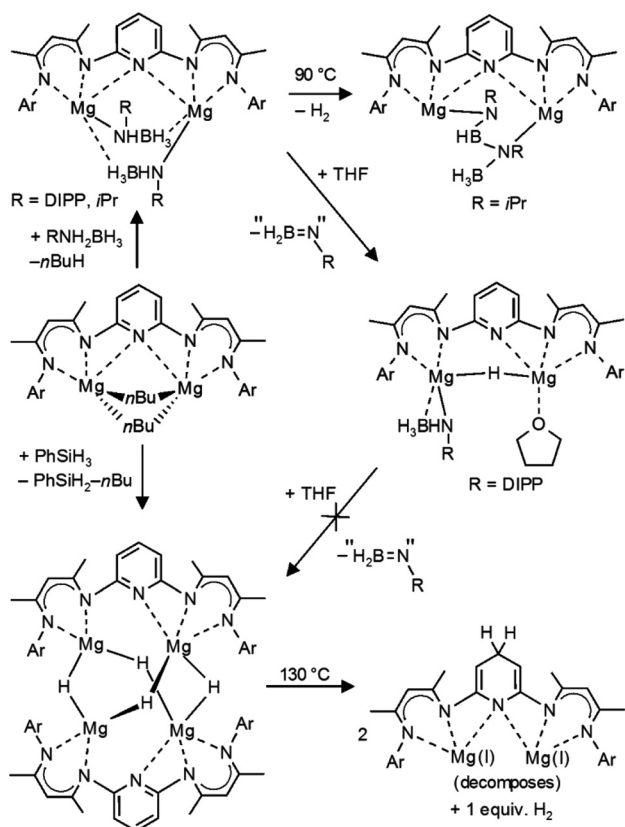
$\text{PYR}[\text{MgNH}(\text{DIPP})\text{BH}_3]_2$ was prepared by careful deprotonation of $\text{H}_2\text{N}(\text{DIPP})\text{BH}_3$ by $\text{PYR}(\text{Mg}n\text{Bu})_2$ at $-78\text{ }^\circ\text{C}$. The low temperature is essential and prevents catalytic decomposition of $\text{H}_2\text{N}(\text{DIPP})\text{BH}_3$ in $[(\text{DIPP})\text{NH}]_2\text{BH}$ and BH_3 , as reported earlier.²⁵ The product, which could be isolated in the form of yellow block-like crystals (56%), has been characterized by crystal structure determination (Fig. 1a, Table 1). Its structure is similar to that of $\text{PYR}[\text{MgNH}(i\text{Pr})\text{BH}_3]_2$ and shows a near C_2 -symmetric complex with two B,N-bridging amidoborane anions. Their $\text{Mg}\cdots\text{H}$, $\text{Mg}\cdots\text{B}$ and $\text{Mg}\cdots\text{N}$ distances average 2.10(2) Å, 2.546(2) Å and 2.126(1) Å, respectively, and are similar to those in the $i\text{Pr}$ -substituted complex.²³

The pyridylene bridge is symmetrically bridging the two Mg ions with rather long distances of 2.7–2.8 Å.

^1H NMR signals for $\text{PYR}[\text{MgNH}(\text{DIPP})\text{BH}_3]_2$ in toluene- d_8 are, at room temperature, rather broad. Cooling the sample to $-50\text{ }^\circ\text{C}$ gives a set of sharp signals which allow for unambiguous NMR characterization. The NH and BH_3 groups show broad ^1H NMR signals at 3.13 ppm and 2.28 ppm, respectively. The $i\text{Pr}$ groups in the ligand give rise to four doublet and two septet resonances and the same was found for the $i\text{Pr}$ groups in the $\text{NH}(\text{DIPP})\text{BH}_3^-$ ion.

In contrast to a toluene solution of $(\text{DIPPnacnac})\text{MgNH}(\text{DIPP})\text{BH}_3$, which decomposes into $(\text{DIPPnacnac})\text{MgN}(\text{DIPP}) = \text{BH}_2$ and H_2 at forced conditions (120 °C, 24 hours),²³





Scheme 3 Synthesis and decomposition of $[\text{PYR}-(\text{MgH})_2]_2$.

a toluene solution of $\text{PYR}[\text{MgNH}(\text{DIPP})\text{BH}_3]_2$ already decomposes slowly at room temperature. A singlet ^1H NMR signal at 4.45 ppm indicates H_2 formation. ^{11}B NMR spectra suggest formation of $[(\text{DIPP})\text{NH}]_2\text{BH}$ and the BH_4^- ion, but well-defined products could not be isolated.

Interestingly, addition of minor amounts of THF to a benzene solution of $\text{PYR}[\text{MgNH}(\text{DIPP})\text{BH}_3]_2$ initiated a fast decomposition reaction and resulted in precipitation of yellow crystals (Scheme 3). Structural characterization of the product revealed the occurrence of a single β -H elimination: $\text{PYR}[\text{MgNH}(\text{DIPP})\text{BH}_3](\text{MgH})\cdot\text{THF}$. The crystal structure (Fig. 1b, Table 1) shows a binuclear molecule with symmetrical bridging of H^- between the Mg^{2+} centers: 1.93(3) Å and 1.95(2) Å. The remaining amidoborane anion binds only to Mg1. This unsymmetrical charge distribution of anions is balanced by strong coordination of the pyridylene bridge to Mg2 (2.199(2) Å) and an additional THF ligand.

^1H NMR signals can be assigned unambiguously: the amidoborane part shows a broad BH_3 signal at 1.58 ppm and a quartet for NH at 2.61 ppm ($^3J(\text{H},\text{H}) = 3.4$ Hz) whereas the bridging H^- gives a singlet at 3.21 ppm.

The mechanism for the here observed THF-induced β -H elimination is subject of speculation. In light of the fact that the preliminary step for β -hydrogen elimination generally requires a low-coordinate metal center with an agostic $\beta\text{-H}\cdots\text{metal}$ contact,²⁶ addition of THF should rather

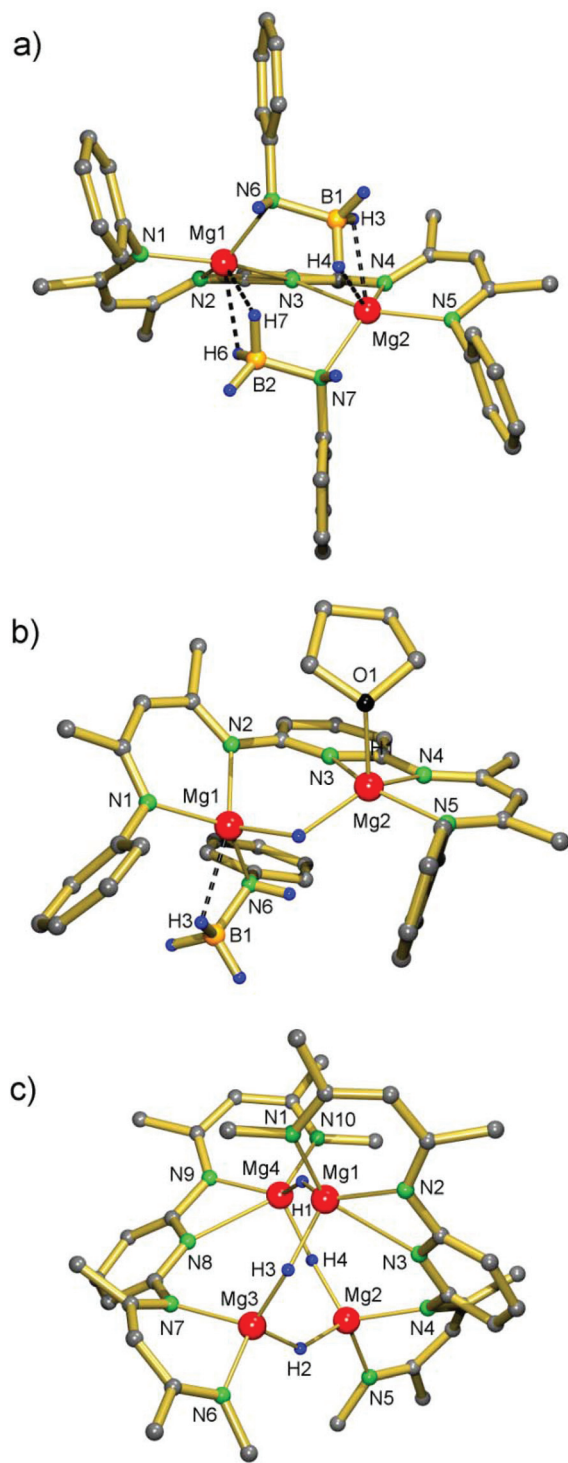


Fig. 1 Crystal structures of (a) $\text{PYR}[\text{MgNH}(\text{DIPP})\text{BH}_3]_2$, (b) $\text{PYR}[\text{MgNH}(\text{DIPP})\text{BH}_3](\text{MgH})\cdot\text{THF}$ and (c) $[\text{PYR}-(\text{MgH})_2]_2$. In all cases, the *iPr* substituents of the DIPP are not shown for clarity (for $[\text{PYR}-(\text{MgH})_2]_2$ only the C_{ipso} atoms of DIPP are shown).

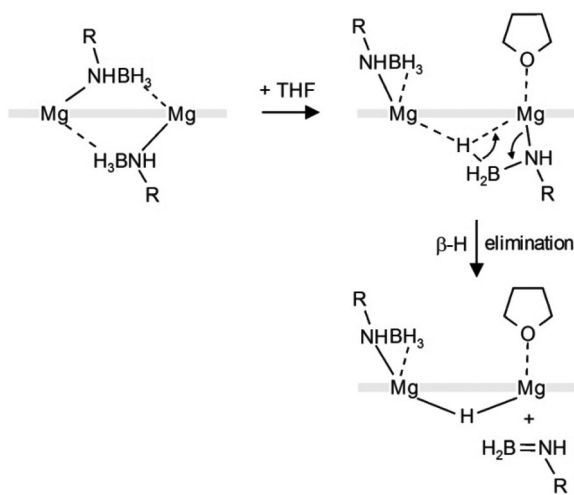
prevent such process. Lewis-base induced β -H eliminations are rare.²⁷

We propose the following reaction sequence (Scheme 4): (i) coordination of THF results in slippage of a bridging amido-



Table 1 Selected distances (Å) for the crystal structures of **PYR**-[MgNH-(DIPP)BH₃]₂, **PYR**-[Mg₂(H)NH(DIPP)BH₃]₂(THF) and **[PYR-(MgH)₂]₂**

PYR -[MgNH(DIPP)BH ₃] ₂			
Mg1–N1	2.085(1)	Mg2...N3	2.701(1)
Mg1–N2	2.031(1)	Mg2–N4	2.039(1)
Mg1...N3	2.780(1)	Mg2–N5	2.093(3)
Mg1–N6	2.121(1)	Mg2–N7	2.130(1)
Mg1...B2	2.538(2)	Mg2...B1	2.554(2)
Mg1...H6	2.21(2)	Mg2...H3	2.22(2)
Mg1...H7	1.98(2)	Mg2...H4	1.97(1)
PYR -[Mg ₂ (H)NH(DIPP)BH ₃] ₂ (THF)			
Mg1–H1	1.95(2)	Mg2–H1	1.93(3)
Mg1–N1	2.081(2)	Mg2–N3	2.199(2)
Mg1–N2	2.093(2)	Mg2–N4	2.068(2)
Mg1–N6	2.093(2)	Mg2–N5	2.119(2)
Mg1...B1	2.649(3)	Mg2–O1	2.029(2)
[PYR-(MgH)₂]₂			
Mg1–H1	1.83(2)	Mg1–N1	2.121(2)
Mg1–H3	1.84(2)	Mg1–N2	2.055(2)
Mg2–H2	1.79(2)	Mg1...N3	2.614(2)
Mg2–H4	1.82(2)	Mg2–N4	2.031(2)
Mg3–H2	1.81(2)	Mg2–N5	2.062(2)
Mg3–H3	1.79(2)	Mg3–N6	2.055(2)
Mg4–H1	1.86(2)	Mg3–N7	2.040(2)
Mg4–H4	1.81(2)	Mg4...N8	2.542(2)
		Mg4–N9	2.052(2)
		Mg4–N10	2.139(2)

**Scheme 4** Proposed mechanism for THF-induced hydride formation; front view (the thick grey line represents **PYR**).

borane ion to terminal coordination and a BH₃ group bridging two Mg²⁺ centers (in fact this intermediate has been observed earlier in the form of the **NN**-[MgNH(*i*Pr)BH₃]₂·THF complex),²³ (ii) this is followed by β-H elimination and formation of the product, (iii) the remaining DIPPN(H) = BH₂ decomposes to [(DIPP)NH]₂BH (detected by ¹¹B NMR) and BH₃ (detected in the form of BH₄[−] by ¹¹B NMR). The last step might go through an intermediate [DIPPN(H)BH₂(DIPP)-NHBH₃][−] anion. Similar intermediates have been isolated in early main group metal and transition metal chemistry.^{25,28–31}

The very mild nature of this Lewis-base induced hydride formation, which is smooth at room temperature, posed the question whether a second H[−] elimination might open a new route for preparation of magnesium hydride complexes. Unfortunately, addition of larger amounts of THF (or using THF as the solvent) did not trigger further β-H elimination. Slowly increasing the temperature of the THF solution led to H₂ formation, presumably by reaction of the Mg–H function with [(DIPP)NH]₂BH, and **PYR**-(MgH)₂ could not be isolated.

Therefore, we chose the slower but more effective phenylsilane route:^{8,9} reaction of a **PYR**-(Mg*n*Bu)₂ solution in benzene with two equivalents of PhSiH₃ gave the product at 60 °C after three days, which could be crystallized from hexane (54%). The crystal structure of the dimer **[PYR-(MgH)₂]₂** shows a near C₂-symmetric tetranuclear cluster without exact crystallographic symmetry (Fig. 1c, Table 1) but with some similarity to **[NN-(MgH)₂]₂**.¹⁴ Although composition and connectivity are similar, the arrangement of Mg ions in **[PYR-(MgH)₂]₂** is strongly distorted from the Mg₄ tetrahedron found in **[NN-(MgH)₂]₂**. Whereas in the latter Mg...Mg distances vary from 3.030(1) to 3.586(1) Å, those in **[PYR-(MgH)₂]₂** are longer and show larger variation: 3.410(1)–4.293(1) Å. This flattened Mg₄ geometry is undoubtedly due to the large span width of the pyridylene bridged **PYR** ligand and results in an 8-membered ring of alternating Mg²⁺ and H[−] ions. However, the average Mg–H distances (H atoms have been located and were refined) are very similar in both structures: **[NN-(MgH)₂]₂** 1.808(9) and **[PYR-(MgH)₂]₂** 1.82(2), but are naturally subject to a large error margin. The pyridylene N atoms are asymmetrically bridging the Mg²⁺ ions with shorter weakly-bound (2.614(2)/2.542(2) Å) and longer essentially non-bonding (3.353(2)/3.407(2) Å) distances. Attempts to incorporate additional MgH₂ into the cluster (*cf.* (iv) in Scheme 2) by reaction of **PYR**-(Mg*n*Bu)₂/(Mg*n*Bu)₂ mixtures with excess PhSiH₃ failed.

The cluster **[PYR-(MgH)₂]₂** contains three different hydride positions (H1, H3/H4 and H2). In case fast pyridyl-Mg1/Mg2 and pyridyl-Mg4/Mg3 switching takes place, at least two different hydride positions are present (H1/H2 and H3/H4). ¹H NMR spectra of **[PYR-(MgH)₂]₂** in toluene-*d*₈, however, only show one singlet for the H[−] ligands. Cooling of the solution to −75 °C did not result in decoalescence. This strongly contrasts with the dynamic behaviour observed for **[NN-(MgH)₂]₂**: below room temperature the singlet hydride signal decoalesces in two triplets.¹⁴ We presume that for **[PYR-(MgH)₂]₂** the solid state structure is maintained in solution but fast dynamics of ligand coordination geometries result in equal hydride positions: a time-averaged structure with symmetrically bridging pyridylene units and flat **PYR** ligands would be S₄-symmetric. This is in agreement with the observation of two *i*Pr doublet signals and one *i*Pr heptet signal. Although a monomeric **PYR**-(MgH)₂ structure with bridging H[−] ligands (type i in Scheme 2) cannot be ruled out, *cf.* **PYR**-(Mg*n*Bu)₂,²³ in apolar solvents it seems the least stable option (especially if one considers the short Mg–H bond distances of 1.8 Å).

The thermal decomposition of yellow crystals of **[PYR-(MgH)₂]₂** was investigated by stepwise heating in a thermo-



stated air-bath. At 130 °C the color changed *via* yellow-orange to dark red. Gas quantification by pumping the gas quantitatively into a calibrated burette of a Töpler pump system indicated the release of 1.1 ± 0.1 mol-equivalents of gas per $[\text{PYR}-(\text{MgH})_2]_2$. Extended heating did not result in more gas elimination. The gas was proven to be H_2 : (i) it does not condense in liquid N_2 but is fully converted to condensable water after leading it over CuO of 300 °C; (ii) after leading the gas in deuterated THF, a clear ^1H NMR resonance could be observed at 4.55 ppm which is the chemical shift for H_2 in this solvent.¹⁸

Thermal H_2 desorption from the $[\text{PYR}-(\text{MgH})_2]_2$ cluster differs from the earlier reported results for $[\text{NN}-(\text{MgH})_2]_2$: hydrogen is released at the significantly lower temperature of 130 °C (*vs.* 175 °C) and only 50% of the theoretical hydrogen content could be detected (*vs.* full conversion). This is likely due to the fact that pyridine is susceptible towards nucleophilic addition of H^- in *ortho*- or *para*-positions to form a de-aromatized amide. Proposed nucleophilic attack at the *para*-position (Scheme 3) explains reduced H_2 release. In contrast to $[\text{NN}-(\text{MgH})_2]_2$, which when dissolved in toluene is stable even after prolonged heating at 150 °C, a toluene solution of $[\text{PYR}-(\text{MgH})_2]_2$ decomposes by a colour change from yellow to dark-red after one hour at this temperature. ^1H NMR analysis indicates de-aromatization of the pyridyl ring, but due to the presence of several different species, no well-defined products could be isolated. We propose initial formation of a dihydropyridide bridged β -diketimate-Mg(I) complex (Scheme 3) which decomposes into various undefined species.

Conclusions

The magnesium hydride chemistry with the 2,6-pyridylene bridged bis- β -diketimate ligand, **PYR**, has been investigated. Although one of the amidoborane anions in $[\text{PYR}-(\text{MgNH}(\text{DIPP})\text{BH}_3)_2]$ could be converted into H^- by a THF-induced β -H elimination, such a transformation could not be achieved for the second amidoborane anion. Reaction of $[\text{PYR}-(\text{Mg}n\text{Bu})_2]$ with PhSiH_3 gave the desired magnesium hydride complex in the form of the dimer $[\text{PYR}-(\text{MgH})_2]_2$. Attempts to incorporate additional MgH_2 into the cluster failed. The structure of $[\text{PYR}-(\text{MgH})_2]_2$ is different from that reported previously for $[\text{NN}-(\text{MgH})_2]_2$, a complex with directly coupled β -diketimate units and four Mg^{2+} ions at the corners of a tetrahedron. Instead, a flattened Mg_4 geometry is found in which alternating Mg^{2+} and H^- ions form an 8-membered ring. $[\text{PYR}-(\text{MgH})_2]_2$ decomposes at 130 °C releasing one equivalent of H_2 . In contrast, $[\text{NN}-(\text{MgH})_2]_2$ decomposes at 175 °C and releases two equivalents of H_2 . It is proposed that nucleophilic attack at the *para*-position explains reduced H_2 formation (Scheme 3). Although the fate of the magnesium is unclear, it is likely that low-valent magnesium species were formed initially. We continue our investigations with the challenging isolation of larger well-defined Mg(I) clusters.

Experimental

General

All experiments were carried out using standard Schlenk-techniques and freshly dried solvents. The following compounds were prepared according to the literature: **PYR**- H_2 ,²² $[\text{PYR}-(\text{Mg}(n\text{Bu}))_2]_2$,²³ $(\text{DIPP})\text{NH}_2\text{BH}_3$.³² NMR spectra were measured using a Bruker DPX300 and DRX500 spectrometer. Crystals were measured using a Siemens Smart diffractometer with APEXII area detector system.

Syntheses

$[\text{PYR}-(\text{MgNH}(\text{DIPP})\text{BH}_3)_2]$. 408 mg (0.542 mmol) $[\text{PYR}-(\text{Mg}(n\text{Bu}))_2]$ was dissolved in 10 mL of toluene and the solution was cooled to -78 °C in an *i*PrOH/ CO_2 cooling bath. At this temperature, a solution of 207 mg (1.08 mmol) $(\text{DIPP})\text{NH}_2\text{BH}_3$ in 2 mL of toluene was added slowly. The reaction mixture was stirred and the cooling bath slowly warmed to room temperature overnight. The solution was concentrated to half its volume and slowly cooled to -27 °C. The product $[\text{PYR}-(\text{MgNH}(\text{DIPP})\text{BH}_3)_2]$ was crystallized in the form of large yellow blocks. Yield: 310 mg, 0.304 mmol, 56%. Elemental analysis (%) calcd for $\text{C}_{63}\text{H}_{93}\text{B}_2\text{Mg}_2\text{N}_7$ ($M_r = 1018.69$): C 74.28, H 9.20; found C 74.48, H 9.00.

$^1\text{H}\{^{11}\text{B}\}$ NMR (500 MHz, toluene- d_8 , -40 °C): $\delta = 0.19$ (d, $^3J(\text{H,H}) = 6.3$ Hz, 6H, *i*Pr), 0.62 (d, $^3J(\text{H,H}) = 6.2$ Hz, 6H, *i*Pr), 0.86 (d, $^3J(\text{H,H}) = 6.5$ Hz, 6H, *i*Pr), 0.95 (d, $^3J(\text{H,H}) = 6.3$ Hz, 6H, *i*Pr), 1.19 (d, $^3J(\text{H,H}) = 6.0$ Hz, 6H, *i*Pr), 1.25 (d, $^3J(\text{H,H}) = 6.5$ Hz, 6H, *i*Pr), 1.42 (d, $^3J(\text{H,H}) = 6.2$ Hz, 6H, *i*Pr), 1.44 (s, 6H, Me backbone), 1.49 (d, $^3J(\text{H,H}) = 6.0$ Hz, 6H, *i*Pr), 1.98 (s, 6H, Me backbone), 2.28 (br, 6H, BH_3), 2.64 (sept, $^3J(\text{H,H}) = 6.2$ Hz, 2H, *i*Pr), 2.81 (sept, $^3J(\text{H,H}) = 6.3$ Hz, 2H, *i*Pr), 3.13 (br, 2H, NH), 3.17 (sept, $^3J(\text{H,H}) = 6.5$ Hz, 2H, *i*Pr), 3.59 (sept, $^3J(\text{H,H}) = 6.0$ Hz, 2H, *i*Pr), 4.79 (s, 2H, H backbone), 6.34 (d, $^3J(\text{H,H}) = 8.0$ Hz, 2H, aryl), 6.78 (d, $^3J(\text{H,H}) = 6.4$ Hz, 2H, aryl), 6.94 (t, $^3J(\text{H,H}) = 8.0$ Hz, 1H, aryl), 6.97–7.07 (m, 8H, aryl), 7.12 (m, 2H, aryl). ^{11}B NMR (160 MHz, toluene- d_8 , 20 °C): $\delta = -18.0$ (br). ^{13}C NMR (data taken from 2D-spectra, 75 MHz, toluene- d_8 , -40 °C): $\delta = 23.2$ (*i*Pr), 24.6 (*i*Pr), 24.6 (Me backbone), 24.6 (*i*Pr), 24.8 (*i*Pr), 25.0 (*i*Pr), 25.3 (*i*Pr), 25.3 (Me Backbone), 25.9 (*i*Pr), 27.3 (*i*Pr), 27.4 (*i*Pr), 28.3 (*i*Pr), 28.4 (*i*Pr), 29.1 (*i*Pr), 100.0 (backbone), 110.7 (aryl), 122.9 (aryl), 123.7 (aryl), 124.1 (aryl), 124.2 (aryl), 125.2 (aryl), 126.4 (aryl), 138.4 (aryl), 139.7 (aryl), 140.9 (aryl), 142.3 (aryl), 142.3 (aryl), 145.5 (aryl), 145.6 (aryl), 161.1 (aryl), 162.5 (backbone), 173.1 (backbone).

$[\text{PYR}-(\text{Mg}_2(\text{H})\text{NH}(\text{DIPP})\text{BH}_3)_2(\text{THF})]$. 200 mg (0.196 mmol) $[\text{PYR}-(\text{MgNH}(\text{DIPP})\text{BH}_3)_2]$ was dissolved in 3.5 mL of THF. After three hours, yellow crystalline blocks of $[\text{PYR}-(\text{Mg}_2(\text{H})\text{NH}(\text{DIPP})\text{BH}_3)_2(\text{THF})_3]$ were separated. The product was isolated by centrifugation, the mother liquor was removed and subsequently washed with 2.0 mL of hexane and shortly dried in high vacuum. Yield of $[\text{PYR}-(\text{Mg}_2(\text{H})\text{NH}(\text{DIPP})\text{BH}_3)_2(\text{THF})_3]$: 85 mg, 0.081 mmol, 41%. Note that, instead of one THF, three equivalents of THF are included. This is due to cocrystallized non-bonding THF ligands (see below). The mother liquor of the reaction mixture gave another crop of the microcrystalline



product: the solvents were removed under high vacuum and the remaining solid was washed with 2.0 mL of hexane and dried under high vacuum. The combined yields of **PYR**-[Mg₂(H)NH(DIPP)BH₃]₂(THF)₃ are 117 mg, 0.112 mmol, 57%. Crystals for crystal structure determination were obtained by recrystallization from a 5/1 benzene–THF mixture. The constitution is **PYR**-[Mg₂(H)NH(DIPP)BH₃]₂(THF); two disordered benzene molecules instead of THF molecules cocrystallized. Elemental analysis for the first batch of well-defined crystals (%) calcd for C₆₃H₉₇BMg₂N₆O₃ (*M_r* = 1045.90): C 72.35, H 9.35; found C 72.34, H 9.16. ¹H{¹¹B} NMR (500 MHz, THF-*d*₈, 20 °C): δ = 1.06 (d, ³J(H,H) = 6.3 Hz, 12H, *i*Pr NH), 1.08 (br, 12H, *i*Pr), 1.11 (d, ³J(H,H) = 6.4 Hz, 12H, *i*Pr), 1.58 (br, 3H, BH₃), 1.63 (s (br), 6H, Me backbone), 1.78 (m, 12H, THF), 2.13 (s (br), 6H, Me backbone), 2.61 (q (br), ³J(H,H) = 3.4 Hz, 1H, NH), 2.95 (sept, ³J(H,H) = 6.4 Hz, 2H, *i*Pr NH), 3.09 (br, 4H, *i*Pr), 3.21 (s, 1H, MgH), 3.62 (m, 12H, THF), 4.78 (s (br), 2H, H backbone), 6.20 (br, 1H, aryl), 6.59 (br, 2H, aryl NH), 6.69 (d, ³J(H,H) = 6.7 Hz, 2H, aryl NH), 7.00–7.12 (m, 7H, aryl). ¹¹B NMR (160 MHz, THF-*d*₈, 20 °C): δ = -18.1 (br). ¹³C NMR (data taken from 2D spectra, 75 MHz, THF-*d*₈, 20 °C): 24.3 (Me backbone), 25.1 (*i*Pr), 25.2 (*i*Pr), 25.5 (Me backbone), 26.2 (THF), 29.2 (*i*Pr), 29.7 (*i*Pr), 68.2 (THF), 99.2 (backbone), 120.0 (aryl NH), 123.0 (aryl), 124.2 (aryl), 125.8 (aryl), 139.2 (aryl NH), 142.2 (aryl), 146.2 (aryl), 148.6 (aryl), 160.5 (aryl), 161.9 (backbone), 172.1 (backbone).

[**PYR**-(MgH)₂]₂. A solution of phenylsilane (90 mg, 0.832 mmol) and **PYR**-[Mg(*n*Bu)]₂ (300 mg, 0.399 mmol) in 6 mL of benzene was heated to 60 °C for three days. The solvent was removed under high vacuum and the residue was dissolved in 2 mL of hexane. After two days at room temperature yellow crystals formed. Yield: 138 mg, 0.108 mmol, 54%. Elemental analysis (%) calcd for C₇₈H₁₀₆Mg₄N₁₀ (*M_r* = 1280.97): C 73.14, H 8.34; found C 73.36, H 8.38. ¹H NMR (300 MHz, benzene-*d*₆, 20 °C): δ = 0.96 (d, ³J(H,H) = 6.8 Hz, 12H, *i*Pr), 1.16 (d, ³J(H,H) = 7.0 Hz, 12H, *i*Pr), 1.57 (s, 6H, Me backbone), 1.82 (s, 6H, Me backbone), 2.88 (s, 2H, MgH), 3.14 (sept, ³J(H,H) = 6.8 Hz, 4H, *i*Pr), 4.79 (s, 2H, H backbone), 6.12 (d, ³J(H,H) = 7.9 Hz, 2H, aryl), 6.99–7.03 (m, 6H, aryl), 7.03 (t, ³J(H,H) = 7.9 Hz, 1H, aryl). ¹³C NMR (75 MHz, benzene-*d*₆, 20 °C): 24.6 (Me backbone), 24.6 (*i*Pr), 24.7 (Me backbone), 25.0 (*i*Pr), 28.6 (*i*Pr), 99.7 (backbone), 111.3 (aryl), 124.1 (aryl), 125.7 (aryl), 138.1 (aryl), 142.4 (aryl), 146.1 (aryl), 162.5 (aryl), 164.0 (aryl), 170.8 (backbone).

Crystal structure determinations

The structures were solved by direct methods (SHELXS-97)³³ and refined with SHELXL-97.³⁴ All geometry calculations and graphics were performed with PLATON.³⁵

PYR-[MgNH(DIPP)BH₃]₂. Measurement at -170 °C (MoK α), formula [(C₆₃H₉₃B₂Mg₂N₇), 3.5(C₆H₆)], *M_w* = 1292.06, triclinic, *a* = 14.5633(10) Å, *b* = 15.0972(10) Å, *c* = 20.1383(12) Å, α = 88.321(2)°, β = 71.161(2)°, γ = 68.872(2)°, *V* = 3889.8(4) Å³, space group *P* $\bar{1}$, *Z* = 2, ρ_{calc} = 1.103 g cm⁻³, $\mu(\text{MoK}\alpha)$ = 0.078 mm⁻¹, 53 697 measured reflections, 15 620 independent reflections (*R*_{int} = 0.029), 12 390 reflections observed with

I > 2 σ (*I*), θ_{max} = 26.4°, *R* = 0.0401, *wR*₂ = 0.1043, GOF = 1.03, 1128 parameter, min/max residual electron density -0.30/+0.44 e Å⁻³. Cocrystallized solvent molecules, 3.5 molecules of benzene, were relatively well-ordered and refined anisotropically. All hydrogen atoms, except those of cocrystallized benzene molecules, were found in the difference-Fourier map and were refined isotropically. Hydrogen atoms on the benzene molecules were placed on idealized calculated positions.

PYR-[Mg₂(H)NH(DIPP)BH₃]₂(THF). Measurement at -156 °C (MoK α), formula [C₅₅H₈₁BMg₂N₆O], *M_w* = 901.69, orthorhombic, *a* = 13.4280(7) Å, *b* = 20.4076(10) Å, *c* = 21.3571(10) Å, *V* = 5852.6(5) Å³, space group *P*2₁2₁2₁, *Z* = 4, ρ_{calc} = 1.023 g cm⁻³, $\mu(\text{MoK}\alpha)$ = 0.080 mm⁻¹, 20 850 measured reflections, 10 889 independent reflections (*R*_{int} = 0.038), 9207 reflections observed with *I* > 2 σ (*I*), θ_{max} = 26.5°, *R* = 0.0480, *wR*₂ = 0.1260, GOF = 1.06, 621 parameter, min/max residual electron density -0.24/+0.61 e Å⁻³. Two cocrystallized molecules of heavily disordered benzene were treated by the SQUEEZE procedure incorporated in PLATON (214 Å³, 98 e).¹⁵ The hydride and hydrogens on N and B were found in the difference-Fourier map and refined isotropically. All other hydrogen atoms have been placed on calculated positions and were refined in a riding mode. The correct handedness of the chiral unit cell has been checked by refinement of the Flack parameter to 0.01 with esd 0.18.

[**PYR**-(MgH)₂]₂. Measurement at -170 °C (MoK α), formula [(C₇₈H₁₀₆Mg₄N₁₀)], *M_w* = 1280.97, monoclinic, *a* = 24.0463(16) Å, *b* = 15.4013(10) Å, *c* = 22.4206(15) Å, β = 103.909(4)°, *V* = 8059.9(9) Å³, space group *P*2₁/*c*, *Z* = 4, ρ_{calc} = 1.056 g cm⁻³, $\mu(\text{MoK}\alpha)$ = 0.090 mm⁻¹, 83 576 measured reflections, 15 303 independent reflections (*R*_{int} = 0.077), 15 303 reflections observed with *I* > 2 σ (*I*), θ_{max} = 25.8°, *R* = 0.0487, *wR*₂ = 0.1165, GOF = 0.94, 1228 parameter, min/max residual electron density -0.24/+0.43 e Å⁻³. Heavily disordered cocrystallized solvent was treated by the SQUEEZE procedure incorporated in PLATON (290 Å³, 52 e).¹⁵ One of the *i*Pr groups shows rotational disorder over two positions that were refined isotropically. Hydrogen atoms were found in the difference-Fourier map and were refined isotropically, except for those on the disordered *i*Pr group. The latter were placed on idealized positions and refined in a riding mode.

Crystallographic data (excluding structure factors) have been deposited with the Cambridge Crystallographic Data Centre as supplementary publication no. CCDC 992444–992446 for **PYR**-[MgNH(DIPP)BH₃](MgH)·THF, **PYR**-[MgNH(DIPP)BH₃]₂, and [**PYR**-(MgH)₂]₂, respectively.

Acknowledgements

The DFG is gratefully acknowledged for financial support. Prof. R. Boese and D. Bläser are thanked for measuring X-ray data and H. Bandmann for measuring the 500 MHz NMR spectra.



Notes and references

- 1 G. S. McGrady and G. Guilera, *Chem. Soc. Rev.*, 2003, **32**, 383.
- 2 S. Aldridge and A. J. Downs, *Chem. Rev.*, 2001, **101**, 3305.
- 3 P. Rittmeyer and U. Wietelmann, Hydrides, in *Ullmann's Encyclopedia of Industrial Chemistry*, Wiley-VCH, 2012, p. 103.
- 4 S. Harder, *Chem. Commun.*, 2012, **48**, 11165.
- 5 D. Hoffmann, T. Kottke, R. J. Lagow and R. D. Thomas, *Angew. Chem., Int. Ed.*, 1998, **37**, 1537.
- 6 D. R. Armstrong, W. Clegg, R. P. Davies, S. T. Liddle, D. J. Linton, P. R. Raithby, R. Snaith and A. E. H. Wheatley, *Angew. Chem., Int. Ed.*, 1999, **38**, 3367.
- 7 D. J. Gallagher, K. W. Henderson, A. R. Kennedy, C. T. O'Hara, R. E. Mulvey and R. B. Rowlings, *Chem. Commun.*, 2002, 376.
- 8 S. Harder and J. Brettar, *Angew. Chem., Int. Ed.*, 2006, **45**, 3474.
- 9 S. P. Green, C. Jones and A. Stasch, *Angew. Chem., Int. Ed.*, 2008, **47**, 9079.
- 10 M. Arrowsmith, M. S. Hill, D. J. MacDougall and M. F. Mahon, *Angew. Chem., Int. Ed.*, 2009, **48**, 4013.
- 11 S. Harder, J. Spielmann, J. Intemann and H. Bandmann, *Angew. Chem., Int. Ed.*, 2011, **50**, 4156.
- 12 (a) A. Stasch, *Angew. Chem., Int. Ed.*, 2012, **51**, 1930; (b) C. Appelt, J. C. Sloopweg, K. Lammertsma and W. Uhl, *Angew. Chem., Int. Ed.*, 2012, **51**, 5911.
- 13 P. Jochmann, J. P. Davin, T. P. Spaniol, L. Maron and J. Okuda, *Angew. Chem., Int. Ed.*, 2012, **51**, 2098.
- 14 J. Intemann, J. Spielmann, P. Sirsch and S. Harder, *Chem. – Eur. J.*, 2013, **19**, 8478.
- 15 A. Stasch, *Angew. Chem., Int. Ed.*, 2014, **53**, 1338.
- 16 F. Buch, J. Brettar and S. Harder, *Angew. Chem., Int. Ed.*, 2006, **45**, 2741.
- 17 J. Spielmann, F. Buch and S. Harder, *Angew. Chem., Int. Ed.*, 2008, **47**, 9434.
- 18 S. Harder, *Chem. Rev.*, 2010, **110**, 3852.
- 19 A. G. M. Barrett, M. R. Crimmin, M. S. Hill and P. A. Procopiu, *Proc. R. Soc. London, Ser. A.*, 2010, **466**, 927.
- 20 S. J. Bonyhady, D. Collis, G. Frenking, N. Holzmann, C. Jones and A. Stasch, *Nat. Chem.*, 2010, **2**, 865.
- 21 R. W. P. Wagemans, J. H. van Lenthe, P. E. de Jongh, A. J. van Dillen and K. P. de Jong, *J. Am. Chem. Soc.*, 2005, **127**, 16675.
- 22 D. F.-J. Piesik, S. Range and S. Harder, *Organometallics*, 2008, **27**, 6178.
- 23 J. Spielmann, D. F.-J. Piesik and S. Harder, *Chem. – Eur. J.*, 2010, **16**, 8307.
- 24 H. Gehring, R. Metzinger, C. Hertwig, J. Intemann, S. Harder and C. Limberg, *Chem. – Eur. J.*, 2013, **19**, 1629.
- 25 J. Spielmann, M. Bolte and S. Harder, *Chem. Commun.*, 2009, 6934.
- 26 (a) P. S. Braterman and R. J. Cross, *Chem. Soc. Rev.*, 1973, **2**, 271; (b) G. F. Schmidt and M. Brookhart, *J. Am. Chem. Soc.*, 1985, **107**, 1443; (c) B. J. Burger, M. E. Thompson, W. D. Cotter and J. E. Bercaw, *J. Am. Chem. Soc.*, 1990, **112**, 1566.
- 27 (a) K. Yan, J. J. D. Heredia, A. Ellern, M. S. Gordon and A. D. Sadow, *J. Am. Chem. Soc.*, 2013, **135**, 15225; (b) D. Mukherjee, A. Ellern and A. D. Sadow, *J. Am. Chem. Soc.*, 2010, **132**, 7582.
- 28 D. J. Liprot, M. S. Hill, M. F. Mahon and D. J. MacDougall, *Chem. – Eur. J.*, 2010, **16**, 8508.
- 29 T. B. Marder, *Angew. Chem., Int. Ed.*, 2007, **46**, 8116.
- 30 C. W. Hamilton, R. T. Baker, A. Staubitz and I. Manners, *Chem. Soc. Rev.*, 2009, **38**, 27.
- 31 D. Y. Kim, N. J. Singh, H. M. Lee and K. S. Kim, *Chem. – Eur. J.*, 2009, **15**, 5598.
- 32 J. Spielmann and S. Harder, *J. Am. Chem. Soc.*, 2009, **131**, 5064.
- 33 G. M. Sheldrick, *SHELXS-97, Program for Crystal Structure Solution*, Universität Göttingen, Göttingen (Germany), 1997.
- 34 G. M. Sheldrick, *SHELXL-97, Program for Crystal Structure Refinement*, Universität Göttingen, Göttingen (Germany), 1997.
- 35 A. L. Spek, *Platon, A Multipurpose Crystallographic Tool*, Utrecht (The Netherlands), 2000.

